Journal of Molecular Structure 1254 (2022) 132344

Contents lists available at ScienceDirect

Journal of Molecular Structure

journal homepage: www.elsevier.com/locate/molstr

Effective removal of phenol by activated charcoal/BiOCl composite under UV light irradiation

Nikita Sharma[a,b,*], Zsolt Pap[a,c], Baán Kornélia[a], Tamas Gyulavari[a], Gábor Karacs[d], Zoltan Nemeth[b], Seema Garg[e], Klara Hernadi[a,f,*]

[a] Department of Applied and Environmental Chemistry, University of Szeged, H–6720 Rerrich Béla 1, Szeged, Hungary
[b] Advanced Materials and Intelligent Technologies Higher Education and Industrial Cooperation Centre, University of Miskolc, Miskolc H-3515, Hungary
[c] Nanostructured Materials and Bio-Nano-Interfaces Centre, Institute for Interdisciplinary Research on Bio-Nano-Sciences, Babeş–Bolyai University, RO400271, Treboniu Laurian 42, Cluj-Napoca, Romania
[d] MTA-ME Materials Science Research Group, ELKH, H-3515 Miskolc Egyetemváros, Hungary
[e] Department of Chemistry, Amity Institute of Applied Sciences, Amity University, Sector-125, Noida U.P. 201313, India
[f] Metal Forming and Nanotechnology, Institute of Physical Metallurgy, University of Miskolc, HU-3515 Miskolc-Egyetemváros C/1 108, Miskolc, Hungary

ARTICLE INFO

Article history:
Received 20 October 2021
Revised 28 December 2021
Accepted 4 January 2022
Available online 6 January 2022

Keywords:
Bismuth oxychloride
Activated charcoal
Phenol
Composites
Photodegradation

ABSTRACT

In this work, composites of BiOCl with activated carbon (AC) were prepared *via* hydrothermal synthesis under environmentally benign conditions using water as solvent. The as-prepared samples were then characterized by using different techniques such as X-Ray Diffraction (XRD) Scanning Electron Microscopy (SEM), Energy Dispersive X-Ray Spectroscopy (EDX), Raman Spectroscopy and UV–Vis Diffuse Reflectance Spectroscopy. The different compositions of AC were used for the synthesis of BiOCl composites (0.5 wt.% and 1 wt.%) to study the removal efficiency of the composites for phenol as model pollutant. Through the photocatalytic degradation results, it was found that more than half of the phenol was photodegraded by AC/BiOCl composites in only 120 min under UV light irradiation. The AC decreased the primary crystallite size and band gap of the samples which further supports the high performance of AC/BiOCl composites than pure BiOCl under UV light irradiation.

1. Introduction

BiOCl is a novel and promising candidate in the field of photocatalysis, like other BiOX. It is a white-colored semiconductor and was the first among other BiOXs to be studied for its photocatalytic properties in 2006 by Zhang et al. [1]. Since then it has received much attention for its potential applications as a novel photocatalyst. It is due to its unique layered structure that imparts high photocatalytic activity and chemical stability. Similar to other BiOXs, BiOCl crystallizes into tetragonal matlockite structure which consists of Bi_2O_2 slabs interleaved by double chlorine atom slabs forming a layered structure. Each [Cl-Bi-O-Bi-Cl] layer contains a bismuth atom surrounded by four oxygen and four chlorine atoms. BiOCl has a wide band gap (~3.2–3.5 eV) which is quite close to the classically-known photocatalyst, TiO_2 (Eg: ~3.0–3.2 eV), therefore, it is UV active [2,3]. Although dye-sensitized BiOCl have shown good response for the photodegradation of RhB under visible light [4,5]. Upon irradiation, BiOCl generates electron/hole pairs which further participate in redox reactions and carry out the photodegradation of pollutants. Their application covers a broad spectrum in photocatalytic energy conversion and environmental remediation area, such as hydrogen production by solar water splitting, indoor-gas purification, photocatalytic wastewater treatment, photodegradation of volatile organic compounds (VOC) and nitrogen fixation. But there are still two main drawbacks of BiOCl that need to be addressed. Firstly, synthesizing this material through an environmentally friendly route and secondly, its limited light absorption and energy loss resulting from the recombination of photogenerated electron/hole pairs. Hence, alone it would not serve the role of an efficient photocatalyst at industrial level. Thus, exploring new strategies to optimize its photocatalytic activ-

* Corresponding authors at: Department of Applied and Environmental Chemistry, University of Szeged, H–6720 Rerrich Béla 1, Szeged, Hungary.
E-mail addresses: nikita.sharma@uni-miskolc.hu (N. Sharma), gyulavarit@chem.u-szeged.hu (T. Gyulavari), hernadi@chem.u-szeged.hu (K. Hernadi).

https://doi.org/10.1016/j.molstruc.2022.132344

ity remains a necessity. Considerable efforts have been put in this regard to enhance its photocatalytic response. Some of the techniques may include tuning of morphology or crystal orientation via controlled synthesis, use of co-catalyst, forming heterojunctions, doping or forming composites based on carbon or nitrogen or noble metals. Among these, we found a limited number of studies reported for carbon-based composites with BiOX unlike in the case of TiO_2 which consists of a huge pile of work in carbon-based composite system.

Activated Charcoal is one of the cheap and readily available materials. It is also sometimes called active carbon or activated carbon and is a class of carbon nanostructures which has been widely used since long as a support or adsorbent in case of removal of pollutants from air [6] or eliminating organic amides from aqueous solutions [7]. Owing to its large adsorption capacity, it is one of the common choices for adsorbents in industries as the intermediates produced after photodegradation process can be effectively adsorbed on its surface. Like with other carbon nanostructures, the combination of AC with semiconductor can suppress the recombination of electron/hole pairs to some extent. It is also the most preferred choice in case of carbon-supported catalysts [8]. However, its adsorptive property alone would not be sufficient if the main application involves mineralization of organic pollutants because the removal of pollutants using AC is primarily based on surface adsorption. Therefore, the studies on composites of semiconductor photocatalyst with AC are carried out to exploit the benefits of each of these materials.

Herein, we report a simple and environmentally benign method to prepare the composites of BiOCl and activated carbon *via* hydrothermal synthesis. Further investigation of their photocatalytic efficiency for the removal of phenol under UV light irradiation was carried out.

2. Materials and methods

2.1. Materials

Following reagents were used as precursors: Bismuth nitrate pentahydrate (VWR, 98.0%), glacial acetic acid (Molar Chemicals Kft. 99.9%), potassium chloride (VWR, 98.0%), Activated Charcoal (Sigma Aldrich, 100 mesh) and phenol (VWR, analytical grade). All the reagents used in this study were of analytical grade and used without further purification. For the synthesis and photocatalytic experiments, ultrapure *Millipore Milli-Q* (MQ) water was used.

2.2. Method

2.2.1. Synthesis of AC/BiOCl composites

Two solutions A and B were prepared and used for the synthesis of BiOCl and AC/BiOCl composites. For solution A, 3 g $Bi(NO_3)_3{\cdot}5H_2O$ was dissolved in 3 mL glacial acetic acid with continuous magnetic stirring and heated around 45 °C to speed up the mixing process in order to obtain a homogenized solution. After this, a calculated amount of AC and 25 mL of deionized water was added and sonicated for an hour. The following wt.% composition of AC was taken: 0.5 and 1 wt.%. This was marked as solution A. For solution B, 0.46 g potassium chloride (KCl) was dissolved in 25 mL deionized water and mixed thoroughly. Solution B was added dropwise to solution A with continuous magnetic stirring and the mixture was stirred for another 30 min. It was then transferred to 120 mL Teflon®-lined stainless-steel autoclave and subjected to 150 °C for 6.30 h. The mixture was cooled down naturally to room temperature and the product was collected and washed with ethanol and deionized water three times and dried in the oven around 40 °C overnight. The similar process was followed for the synthesis of pure BiOCl without activated carbon. This was used as a reference sample. Based on our previous studies, the as-mentioned synthesis conditions were used [9,10].

2.2.2. Characterization

The products were characterized by X-Ray diffraction (XRD) using a Rigaku Miniflex II diffractometer ($2\theta^\circ$ = 10–70°) at λ (CuK_α) = 0.15418 nm equipped with a graphite monochromator for the analysis of the structural properties of the composites, such as the degree of crystallinity and crystal orientations. The mean primary crystallite size was also calculated for the samples using the Scherrer equation [11]. N_2 adsorption-desorption measurements were carried out to measure the specific surface areas of the samples for which a BELCAT-A (Osaka, Japan) device was used and calculated according to the BET (Brunauer-Emmett-Teller) method. Morphological analysis was carried out using Scanning Electron Microscopy (SEM), Hitachi S-4700 Type II FE-SEM (Tokyo, Japan) instrument operating using a cold field emission gun (5–15 kV) and Transmission Electron Microscopy (TEM). For TEM measurements, the as-prepared samples were examined by high-resolution transmission electron microscopy (HRTEM, FEI Technai G2 electron microscope, 200 kV) to explore the morphology and particle size of the nanocomposites. Sample preparation was made by dropping an aqueous suspension of the nanocomposites on 300 mesh copper grids (lacey carbon, Ted Pella Inc.). The optical properties were analyzed using Diffuse Reflectance Spectroscopy (DRS) JASCO-V650 with an integration sphere (ILV-724) (λ = 300–800 nm). Raman spectroscopy was used to study the composite formation and crystal defects in the prepared composites. A multilaser confocal Renishaw in Via Reflex Raman spectrometer equipped with a Ren-Cam CCD detector was employed to record the Raman spectra. The 532 nm (green) laser was applied as an excitation source. Using a 0.9 NA objective of 100 × magnification, the Raman spectra were collected. The integration times were 20 s, 1800 lines/mm grating for all spectra, and 10% of the maximum laser intensity – laser power was 20 mW with 4 cm^{-1} was the spectral resolution.

2.2.3. Photocatalytic measurements

The photocatalytic activity of BiOCl and AC/BiOCl composites was measured by studying the photodegradation of phenol aqueous solution under UV light irradiation. In case of UV-A irradiation, 6 × 6 W fluorescence UV-A lamps (*Lightech, Dunakeszi, Hungary*) with 365 nm emission maximum were used. The photocatalyst suspension containing the pollutant was continuously purged with air to keep the dissolved oxygen concentration constant during the whole experiment. The initial concentration of phenol (C_0) was 0.1 mM and the amount of catalyst loaded was 1.0 $g{\cdot}L^{-1}$ with 130 mL total volume of the suspension (V_{susp}). The suspension was ultrasonicated for 5 min to ensure formation of homogeneous suspension. The photocatalyst containing suspension was stirred in dark for 30 min to obtain adsorption/desorption equilibrium. After this the lamps were turned on and the samples were withdrawn at regular time intervals. The total irradiation time was 120 min. The samples collected were centrifuged for 3 min. at 15,000 rpm and filtered with Filtratech 0.25 µm syringe filter. The decrease in concentration of the phenol was measured by HPLC (Merck-Hitachi L-7100) with a low-pressure gradient pump, equipped with a Merck-Hitachi L-4250 UV–Vis detector and a Lichrospher R_p 18 column using a methanol/water (50:50 v/v) mixture as eluent and 210 nm as the detection wavelength. Also, an important observation was made when these composites were sonicated in aqueous solution of phenol for photocatalytic studies. Unlike in our previous experiments with other BiOX and CNT [9,10], in this study, the catalyst particles in AC/BiOCl composites were completely dispersed forming homogeneous suspension indicating its hydrophilic nature. Total organic carbon content of the phenol solution was measured using Analytik Jena Multi N/C 3100.

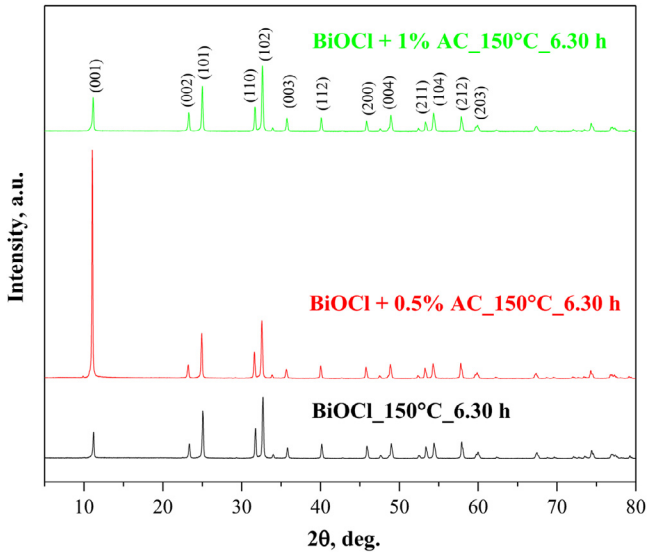

Fig. 1. XRD diffractograms of BiOCl and AC/BiOCl composites prepared at 150 °C for 6:30 h.

3. Results and discussion

3.1. XRD

The XRD patterns of BiOCl and AC/BiOCl composites are shown in Fig. 1. All the diffraction peaks are indexed to the tetragonal phase of BiOCl (JCPDS file no. 06–0249). The main diffraction peak of carbon is not visible due to low amount of AC and overlapping with BiOCl diffraction peak. The diffraction patterns of standard BiOCl crystal did not change after adding AC which means the crystal structure of BiOCl is maintained. Based on our previous studies [10,9], as mentioned in the synthesis section also, in this study we chose the best conditions for obtaining a highly crystalline structure which was the hydrothermal treatment at 150 °C for 6.30 h. This is evident from the diffractograms also, as shown in Fig. 1, where the sharp and intense peaks of AC/BiOCl composites show that the samples are well-crystallized. From Fig. 1, we can see the variation in the peak intensities of (001) and (102) crystal phases. The prepared samples had higher crystallite size as calculated using the Scherrer equation. For pure BiOCl, the crystallite size was more than 100 nm while for the composites a drop in the crystallite size was witnessed. All the composites exhibited primary crystallite size below 100 nm. Therefore, it can be concluded here from these calculations that the presence of AC led to a decrease in primary crystallite size of the composites.

3.2. N_2-adsorption

The specific surface area of the samples was conducted using N_2-adsorption technique and calculated *via* BET (Brunauer-Emmett-Teller) theory. All the prepared samples exhibited lower surface area with the value ranging between 3 and 5 m^2/g. Similar results of low surface area samples were seen in our previous studies of BiOX/CNT composites and yet high photocatalytic activity were reported in such cases. This indicates that in our study surface area is not the determining factor for obtaining high performance of the samples and sometimes, photocatalysts with lower surface area can result in higher photodegradation efficiency. In such cases, other factors such as crystallinity may play a dominant role in deciding the overall photocatalytic efficiency of the photocatalyst.

3.3. SEM and TEM

The morphology of the composites was investigated using scanning electron microscopy. The samples were composed mainly of bulk plates stack on top of each other as shown in Fig. 2. The interesting point to consider here is that in each sample case, whether pure BiOCl or its composite with AC, stacking of these plates was consistent, can be seen in Fig. 2 (a–c). As can be seen from Fig. 2 (a–c), AC is not visible in the SEM images. Therefore, further characterizations were carried out to check their presence. Similar morphology has also been reported in [12]. This kind of nanoplates stacking was also found in our other studies of BiOX composites with CNT [9,10]. One of the possible reasons for this could be the use of water as the solvent in the synthesis process, as reported in [13]. This also explains the low surface area of the samples. In a study by Liu et al., it was reported that use of glacial acetic acid prevented the state of agglomeration because of its low viscosity [14]. Likewise, in this work, water and acetic acid was used for dissolving bismuth precursors, both having lower viscosity than other solvents (like ethylene glycol or glycerin) which allowed BiOCl particles to grow freely, thus avoiding aggregation of nanoplates.

The samples were also investigated by TEM to confirm the presence of AC in the composites. Fig. 3(a) shows the TEM micrographs of AC/BiOCl composites. It was observed, as can be seen from Fig. 3(a), that it is difficult to detect AC, probably, because of its high dispersion. Fig. 3 (b and c) shows morphology of pure AC to confirm that their original particle size does not explain the "invisibility". At higher magnification graphitic-like layered sheets could be seen in Fig. 3(c) marked in circles. The confirmation for presence of these graphitic-like layers is obtained through measuring the interplanar distance (D-spacing) through HRTEM which was around 0.35 nm (shown in the inset of Fig. 3(c)), also coinciding with the literature value [15]. These graphitic sheets represent the presence of sp^2 carbon bonds which would be interesting to verify using a technique which is sensitive to such signals. Therefore, we used Raman spectroscopy to further confirm their presence.

3.4. Raman spectroscopy

Raman measurement was carried out to investigate and confirm the chemical environment of the prepared samples. As depicted

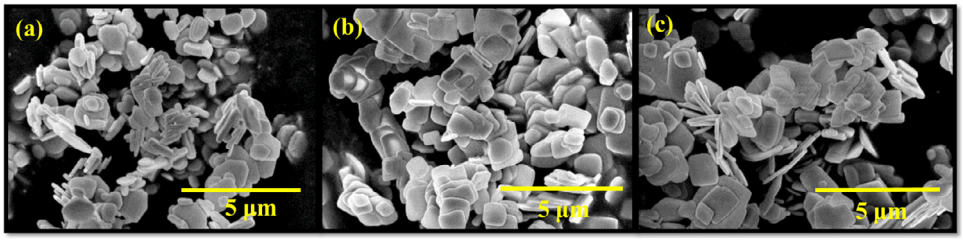

Fig. 2. SEM images of (a) pure BiOCl (b) BiOCl + 0.5% AC (c) BiOCl + 1% AC.

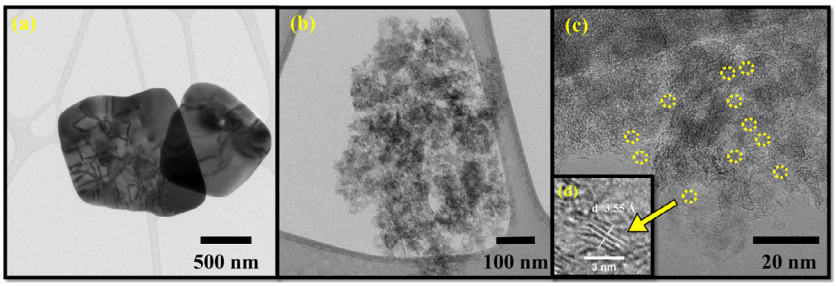

Fig. 3. TEM micrographs of (a) BiOCl + 1%AC (b) pure AC (c) pure AC showing regions reflecting the presence of graphitic-like layered structures *(marked in yellow);* (d) enlarged inset of pure AC showing D-spacing.

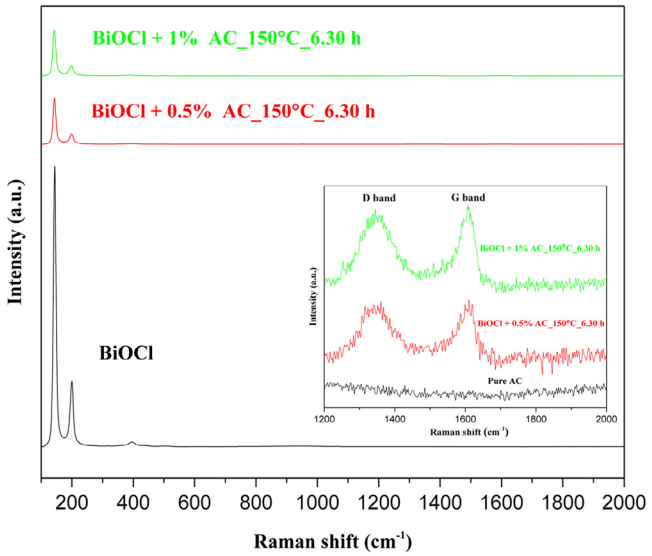

Fig. 4. Raman spectra of BiOCl and AC/BiOCl composites and the inset showing D and G bands of AC.

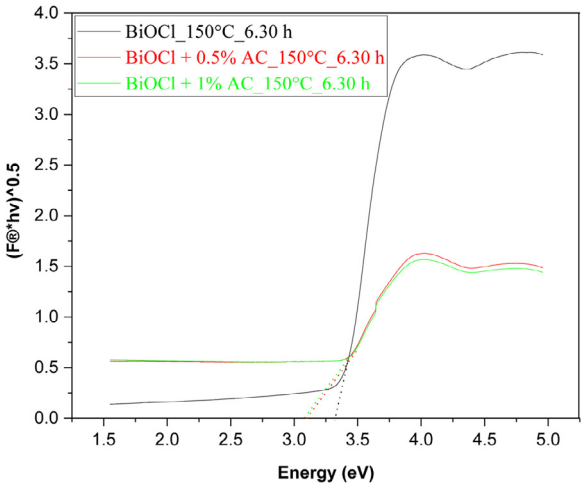

Fig. 5. DRS spectra of the prepared samples at 150 °C and 6.30 h.

in Fig. 4, the peaks at 142, 198, and 392 cm^{-1} were present in all the samples (BiOCl and its composites with various wt.% AC). The strong peak around 142 cm^{-1} corresponds to A_{1g} internal Bi-Cl stretching mode and another peak at 198 cm^{-1} belongs to E_g internal stretching mode of Bi-Cl. A very weak and not readily noticeable peak was also present around 392 cm^{-1} which belongs to E_g and B_{1g} bands due to motion of oxygen atoms. These Raman spectral results are consistent with other previous reports [16,17]. In case of samples containing AC, the bands reflecting sp^2 carbon atoms called D and G bands were also present around 1300–1700 cm^{-1}, however, their intensity varied with change in the amount, as shown in the inset of Fig. 4. The peak at 1350 cm^{-1} represents D band and the peak at 1609 cm^{-1} denotes G band. The presence of D and G bands indicate the successful formation of composites and chemical interaction between AC and BiOCl. Also, the intensity ratio of I_D and I_G bands were calculated which represents the defective nature of carbon present. The initial ratio of I_D/I_G was 0.95 and it increased to 0.97 with increase in AC amount. This represents more defects on the BiOCl surface as a result of different compositions of AC.

3.5. DRS

The photocatalytic activity of a semiconductor is closely related to its band gap energy structure. The optical properties of the composites were, therefore, evaluated using UV–Vis DRS. The indirect band-gap energy was calculated using the Kubelka-Munk equation, that is $[F(R).h\nu]\ p = A(h\nu - E_g)$, where h is Planck constant, E_g is the band gap energy, A is constant and p is dependent on the type of optical transition and is obtained by plotting the graph between $(\alpha h\nu)^{1/2}$ vs. photon energy ($h\nu$). Fig. 5 shows the band gap energy of the samples calculated by Kubelka-Munk (K-M) function. The values follow 3.33, 3.18 and 3.15 eV for samples BiOCl, BiOCl + 0.5% AC, BiOCl + 1% AC, respectively. Through these values, we can see a significant decrease in band gap even with the addition of a very low amount of AC. The pure BiOCl showed strong absorption in the ultraviolet region with an absorption maxima edge near 355 nm.

3.6. Photocatalytic activity

The photocatalytic activity of BiOCl and AC/BiOCl composites was determined by measuring the decomposition rate of phenol in aqueous solution under UV light irradiation in 120 min. The results are summarized in Fig. 6. The dark time for achieving adsorption-desorption equilibrium time was 30 min. During this dark time, negligible phenol adsorption took place since phenol is a poorly adsorbing material. Therefore, the actual decrease in phenol concentration that took place over time is in the presence of light. This indicates the photocatalytic removal of phenol rather than simple adsorption. The removal of phenol gradually increased with the addition of AC. The highest degradation efficiency of 50% was achieved in case of both the composites (0.5 wt.% and 1 wt.% AC) while pure BiOCl reported 40% photodegradaion efficiency under UV light irradiation in 120 min. In the literature, the enhanced photocatalytic activity in case of composites with AC is attributed to the creation of interface between solid phases involved and continuous charge transfer process taking place from AC to semiconductor [18]. Our results look quite promising given the fact that we have used ordinary UV lamps of low power instead of high pres-

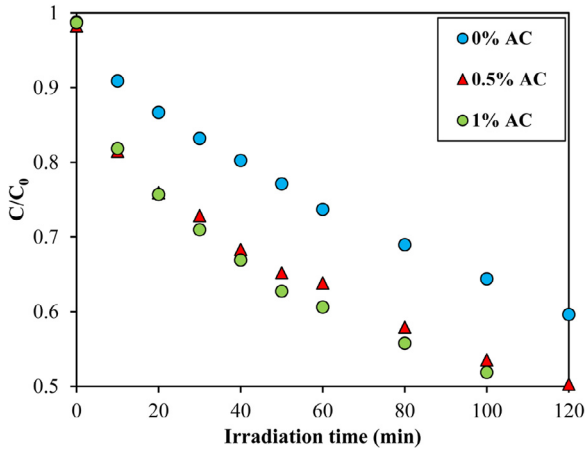

Fig. 6. Photocatalytic Activity of BiOCl and AC/BiOCl towards phenol under UV light irradiation.

sure mercury lamp or Xenon lamps which are not economical options from an industrial point of view. Another interesting point is when we compared our results to a study done by Velasco et al. where immobilization of TiO_2 was done on AC, almost 98% phenol removal was attained after 6 h of irradiation by using high pressure mercury lamps [19]. The enhanced photocatalytic activity of the composites can also be linked to the decreased band gap and primary crystallite size of the composites.

To understand the photocatalytic response of the AC/BiOCl composites, some correlations were studied. Initially, a clear relationship was observed between primary crystallite size of the composites and their photocatalytic activity. As discussed previously in the XRD section, with the addition of AC, a decrease in crystallite size was seen. Following Fig. 7 we can say that increase of crystallite size led to lower photocatalytic activity. This is true because probably less number of active sites are available with higher crystallite size and lower surface area. Further, the correlation between the band gap energy and photodegradation efficiency was also seen. From Fig. 7, it is visible that the band gap energy decreases with the addition of AC which also led to enhanced photocatalytic activity of AC/BiOCl composites as compared to pure BiOCl.

Therefore, in this study we concluded no evidence for the presence of AC from XRD and EM investigations; however, other techniques (Raman, DRS, and photocatalytic activity) revealed the differences between pure BiOCl and their composites with AC. It is assumed that AC might be either dispersed on the surface of BiOCl crystals or trapped inside the nanoplates.

Table 1
TOC values (mg/L) for the sample BiOCl + 1% AC.

Pollutant	TOC value (mg/L)				
	Initial (0 min)	30 min	60 min	90 min	120 min
Phenol	17	15.8	14.6	13.24	11.92

The intermediate investigation of any pollutant is very important, however, some previous studies including our research group, has already dealt with phenol byproducts in detail. From these studies, we can report that phenol upon oxidation generates several intermediates (both aromatic and aliphatic). This is why we proceeded with the TOC measurements to further demonstrate that similar mechanism is valid in our system. For this, the sample with 1% AC composition was selected. As the irradiation time increased, TOC values of the phenol solution decreased gradually. The monotone decrease in TOC values indicates the transformation of phenol although not complete mineralization of the pollutant probably due to shorter decomposition interval as compared to the literature data. The results are shown in Table 1 and Fig. 8 below.

4. Stability

The TOC result for 1% AC composite indicated mineralization of phenol. Meanwhile, we have carried out the stability tests in order to study the structural and morphological changes (if any) in our material. For this, the samples were washed after three cycles with ethanol and water and finally dried for XRD analysis. Fig. 9 illustrates the XRD diffractogram for the samples before and after cycling. The unchanged XRD diffraction patterns after the three runs indicated that BiOCl and BiOCl/AC is structurally stable during the whole photodegradation process. No new peaks were detected in all the samples after three runs of photodegradation test. This indicates that crystal structure of BiOCl has not changed significantly after the tests. From the morphological point of view also, the samples were analysed using SEM before and after the three photocatalytic tests. Fig. 10 shows the SEM micrographs of BiOCl and BiOCl/AC samples before and after the photocatalytic tests. The morphology of the samples has not changed even after the 3 cycles. Similar stacking of nanoplates without any surface irregularities could be seen in Fig. 10. All of these results proves that the catalyst is stable in terms of both, structural and morphological aspects.

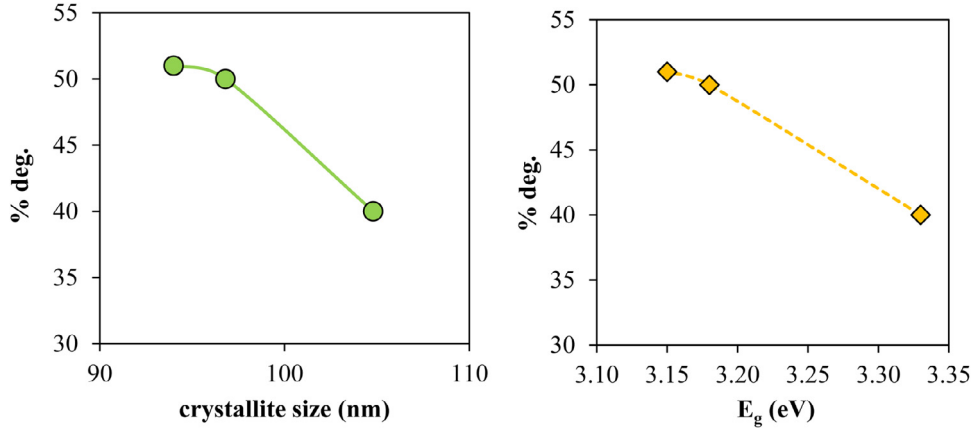

Fig. 7. (a) Correlation between primary crystallite size and photodegradation efficiency (%deg.) of AC/BiOCl composites; (b) Correlation between band gap energy values (E_g) and photodegradation efficiency of AC/BiOCl composites.

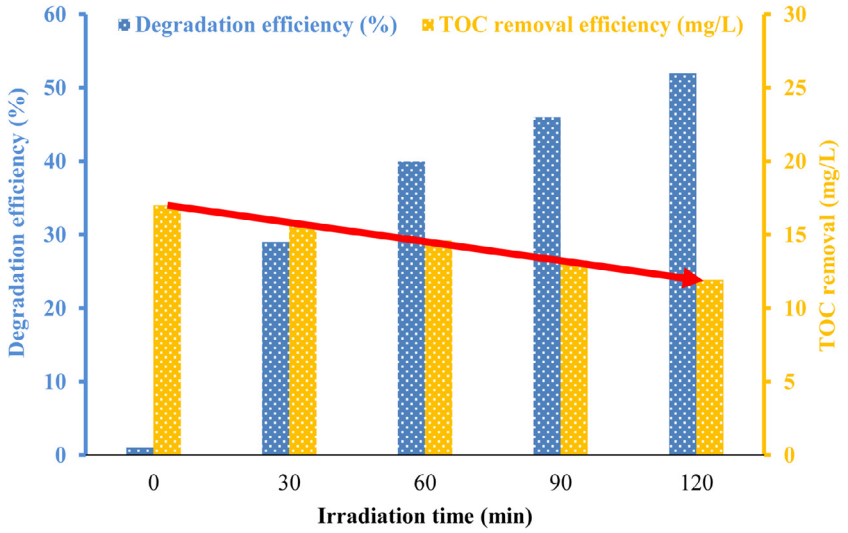

Fig. 8. Photodegradation efficiency (% deg.) and TOC removal (mg/L) for BiOCl + 1% AC composite representing higher degradation efficiency and decrease in TOC values with increasing irradiation time.

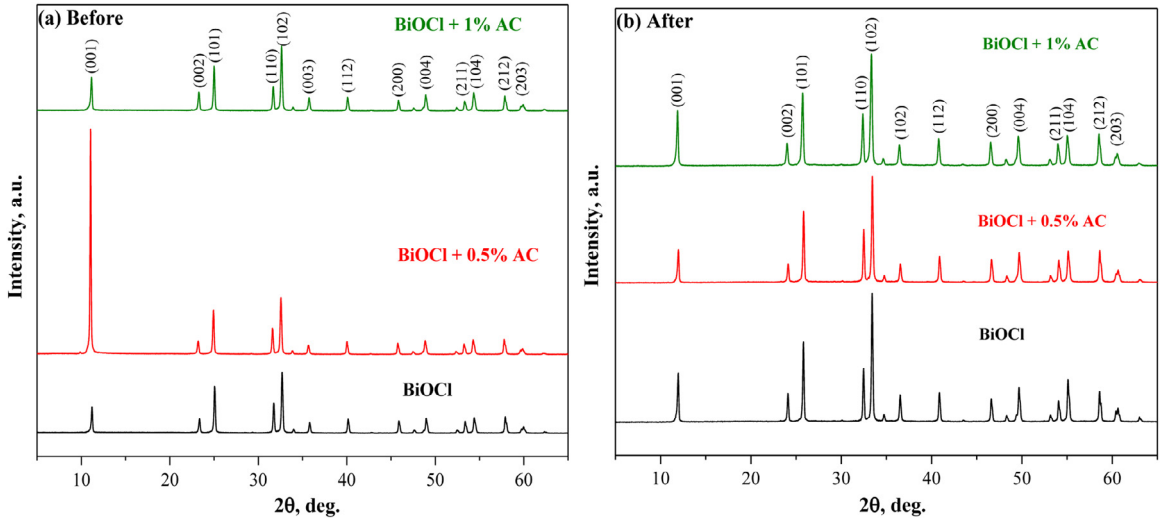

Fig. 9. The diffractograms of BiOCl and BiOCl/AC composites (a) before and (b) after the photocatalytic test (3 cycles).

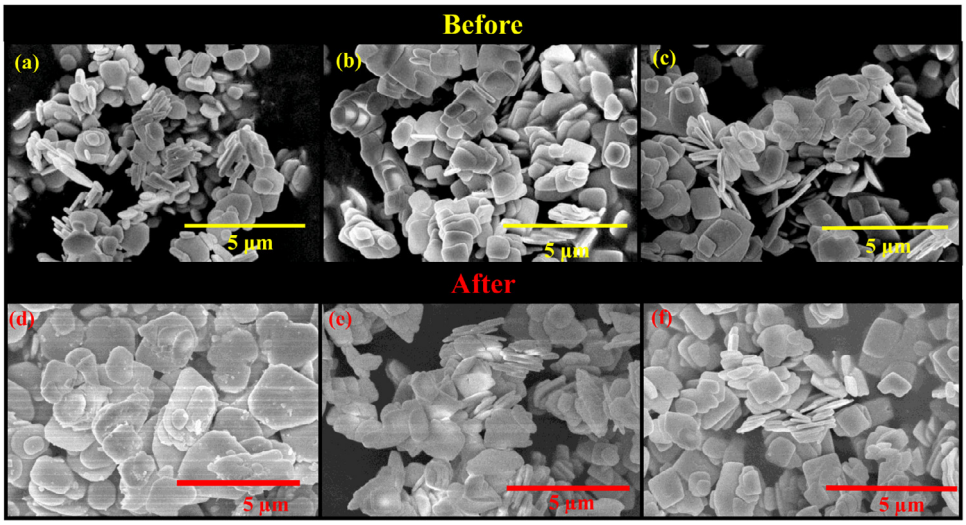

Fig. 10. SEM images of samples before and after the photocatalytic tests. Before photodegradation tests (a) BiOCl, (b) BiOCl + 0.5% AC composites, (c) BiOCl + 1% AC composites; After photodegradation tests (d) BiOCl, (e) BiOCl + 0.5% AC composites, (f) BiOCl + 1% AC composites.

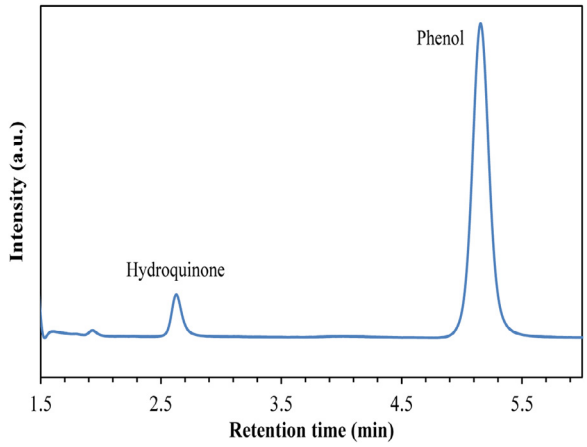

Fig. 11. Chromatogram of BiOCl +1% AC sample showing the signals for phenol and hydroquinone under UV light irradiation (one of the byproduct during photocatalytic degradation of phenol).

4.1. Proposed mechanism

The phenol photodegradation occurs in two steps: intermediate formation and complete mineralization. Clearly, through our results, it is evident that after undergoing irradiation for 2 h, the primary stage intermediates appeared (as evident from Fig. 11). The chromatogram shows the presence of the first intermediate, i.e. hydroquinone, followed by the main peak of phenol. It is known for phenol photodegradation process that the primary intermediate stage involves the formation of catechol, hydroquinone and resorcinol, followed by the ring opening leading to the formation of small molecules of aliphatic organic acids like maleic acid, oxalic acid and formic acid and finally to CO_2 and water. In our study, the TOC constant decreased value shows that the materials are capable of undergoing complete mineralization, if irradiation time is prolonged. Considering literature studies, total mineralization have been reported in the cases of longer irradiation times. For instance, in a study reported by Dang et al., phenol disappeared completely after 24 h of irradiation [20].

It can be assumed that on irradiating the surface of BiOCl particles, the electrons/holes charges are produced and these photogenerated electrons are further migrated to the activated carbon surface due to their good electron conductivity property. In this way, activated carbon is facilitating the charge separation process and hence, enhanced photocatalytic activity could be attained. Fig. 12 represents the scheme for phenol photodegradation by BiOCl/AC composite under UV light irradiation.

5. Conclusion

In the present study, the composites of BiOCl with AC were synthesized *via* hydrothermal synthesis. For the synthesis, the best pre-determined synthesis conditions were used for obtaining higher crystalline material. Two compositions of AC with BiOCl were prepared (0.5 and 1 wt.%). The decrease in the primary crystallite size with the addition of AC was observed. Microplates-like morphology was obtained for all the samples. No morphological transformations took place during composite formation. TEM and Raman spectroscopy confirmed the possible incorporation of AC into BiOCl. The addition of AC also led to a decrease in band gap energy of the AC/BiOCl composites. All of the above-mentioned results facilitated in achieving higher photodegradation efficiency for phenol under UV light. The higher performance for AC/BiOCl composites was obtained (more than 50%) as compared to the pure BiOCl (less than 40%). Additionally, TOC result for BiOCl+1% AC indicates that the material undergo mineralization process which shows that the composite has high potential for the removal of phenol pollutant. The stability tests also demonstrated the structural and morphological stability of the prepared materials. The use of water as media during synthesis demonstrate that the use of non-hazardous solvent can be an effective method for preparing AC/BiOCl photocatalytic material.

Declaration of Competing Interest

The authors declare that they have no known competing financial interests or personal relationships that could have appeared to influence the work reported in this paper.

CRediT authorship contribution statement

Nikita Sharma: Conceptualization, Visualization, Investigation, Writing – original draft, Formal analysis. **Zsolt Pap:** Conceptualization, Visualization, Data curation. **Baán Kornélia:** Investigation. **Tamas Gyulavari:** Investigation, Software. **Gábor Karacs:** Investigation, Data curation. **Zoltan Nemeth:** Investigation, Data curation. **Seema Garg:** Supervision. **Klara Hernadi:** Writing – review & editing, Supervision, Resources.

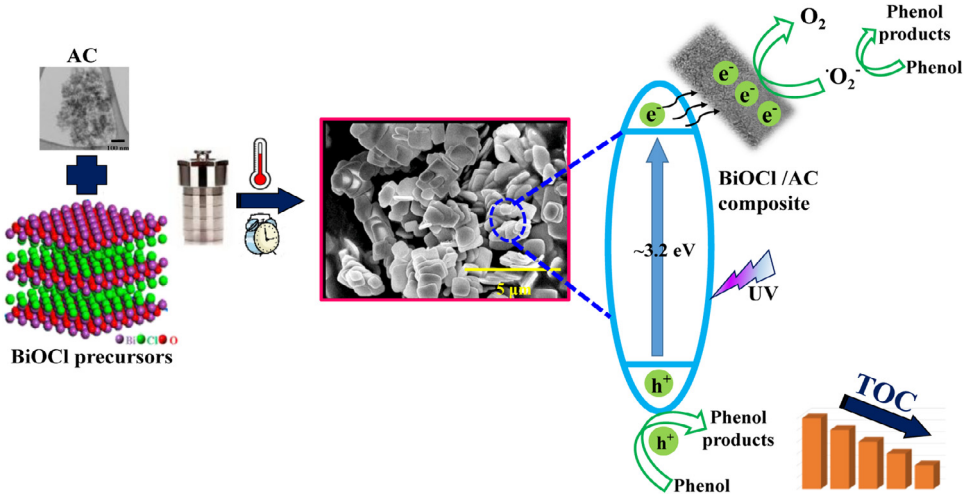

Fig. 12. Schematic representation of photodegradation process of phenol by BiOCl/AC composites.

Acknowledgements

This work was supported by the Indo-Hungarian TÉT project (TÉT_15_IN-1–2016–0013 and Department of Science and Technology, Delhi, India (INT/HUN/P-06/2016). The authors would like to acknowledge the financial support received from Bilateral Scholarship, Tempus Public Foundation, Hungary. Special thanks to my colleagues, Szilvia Fodor, Kovacs Gabor for carrying out SEM and DRS measurements. This research was supported by the European Union and the Hungarian State, co-financed by the European Regional Development Fund in the framework of the GINOP-2.3.4–15–2016–00004 project, aimed to promote the cooperation between higher education and the industry.

References

[1] K.L. Zhang, C.M. Liu, F.Q. Huang, C. Zheng, W.D. Wang, Study of the electronic structure and photocatalytic activity of the BiOCl photocatalyst, Appl. Catal. B Environ. 68 (2006) 125–129, doi:10.1016/j.apcatb.2006.08.002.

[2] R. He, S. Cao, P. Zhou, J. Yu, Recent advances in visible light Bi-based photocatalysts, Chin. J. Catal. 35 (2014) 989–1007, doi:10.1016/s1872-2067(14)60075-9.

[3] H. Zhao, F. Tian, R. Wang, R. Chen, A review on bismuth-related nanomaterials for photocatalysis, Rev. Adv. Sci. Eng. 3 (2014) 3–27, doi:10.1166/rase.2014.1050.

[4] M. Zhao, L.F. Dong, C.D. Li, L.Y. Yu, P. Li, A Facile route to cotton-Like BiOCl nanomaterial with enhanced dye-sensitized visible light photocatalytic efficiency, Chin. Phys. Lett. (2015) 32, doi:10.1088/0256-307X/32/9/098101.

[5] F. Liang, M. Lu, Y.H. Zhang, Q. Shi, F.N. Shi, Synthesis and structure of a bismuth-cobalt bimetal coordination polymer for green efficient photocatalytic degradation of organic wastes under visible light, J. Mol. Struct. 1230 (2021) 129636, doi:10.1016/j.molstruc.2020.129636.

[6] T. Ibusuki, K. Takeuchi, Removal of low concentration nitrogen oxides through photoassisted heterogeneous catalysis, J. Mol. Catal. 88 (1994) 93–102, doi:10.1016/0304-5102(93)E0247-E.

[7] N. Takeda, N. Iwata, T. Torimoto, H. Yoneyama, Influence of carbon black as an adsorbent used in TiO2 photocatalyst films on photodegradation behaviors of propyzamide, J. Catal. 177 (1998) 240–246, doi:10.1006/jcat.1998.2117.

[8] F. Rodriguez-reinoso, The role of carbon materials catalysis * in heterogeneous, 36 (1998) 159–175.

[9] N. Sharma, Z. Pap, I. Székely, M. Focsan, G. Karacs, Z. Nemeth, S. Garg, K. Hernadi, Combination of iodine-deficient BiOI phases in the presence of CNT to enhance photocatalytic activity towards phenol decomposition under visible light, Appl. Surf. Sci. (2021) 565, doi:10.1016/j.apsusc.2021.150605.

[10] N. Sharma, Z. Pap, S. Garg, K. Hernádi, Hydrothermal synthesis of BiOBr and BiOBr/CNT composites, their photocatalytic activity and the importance of early $Bi_6O_6(OH)_3(NO_3)_3{\cdot}1.5H_2O$ formation, Appl. Surf. Sci. 495 (2019) 143536, doi:10.1016/j.apsusc.2019.143536.

[11] U. Holzwarth, N. Gibson, The Scherrer equation versus the “Debye-Scherrer equation”, Nat. Nanotechnol. 6 (2011) 534, doi:10.1038/nnano.2011.145.

[12] F. Duo, Y. Wang, X. Mao, X. Zhang, Y. Wang, C. Fan, A BiPO 4/BiOCl heterojunction photocatalyst with enhanced electron-hole separation and excellent photocatalytic performance, Appl. Surf. Sci. 340 (2015) 35–42, doi:10.1016/j.apsusc.2015.02.175.

[13] J. Li, Y. Yu, L. Zhang, Bismuth oxyhalide nanomaterials: layered structures meet photocatalysis, Nanoscale 6 (2014) 8473–8488, doi:10.1039/c4nr02553a.

[14] H. Liu, J. Huang, J. Chen, J. Zhong, J. Li, D. Ma, Influence of different solvents on the preparation and photocatalytic property of BiOCl toward decontamination of phenol and perfluorooctanoic acid, Chem. Phys. Lett. 748 (2020), doi:10.1016/j.cplett.2020.137401.

[15] N. Yusof, D. Rana, A.F. Ismail, T. Matsuura, Microstructure of polyacrylonitrile-based activated carbon fibers prepared from solvent-free coagulation process, J. Appl. Res. Technol. 14 (2016) 54–61, doi:10.1016/j.jart.2016.02.001.

[16] S. Kang, R.C. Pawar, Y. Pyo, V. Khare, C.S. Lee, Size-controlled BiOCl–RGO composites having enhanced photodegradative properties, J. Exp. Nanosci. 11 (2016) 259–275, doi:10.1080/17458080.2015.1047420.

[17] S. Bunda, V. Bunda, Raman spectra of bismuth oxyhalide single crystals, Acta Phys. Pol. A 126 (2014) 272–273, doi:10.12693/APhysPolA.126.272.

[18] A. Di Paola, E. García-López, G. Marcì, L. Palmisano, A survey of photocatalytic materials for environmental remediation, J. Hazard. Mater. 211–212 (2012) 3–29, doi:10.1016/j.jhazmat.2011.11.050.

[19] L.F. Velasco, J.B. Parra, C.O. Ania, Role of activated carbon features on the photocatalytic degradation of phenol, Appl. Surf. Sci. 256 (2010) 5254–5258, doi:10.1016/j.apsusc.2009.12.113.

[20] T.T.T. Dang, S.T.T. Le, D. Channei, W. Khanitchaidecha, A. Nakaruk, Photodegradation mechanisms of phenol in the photocatalytic process, Res. Chem. Intermed. 42 (2016) 5961–5974, doi:10.1007/s11164-015-2417-3.